Design of Active Disturbance Rejection Control for Single-Link Flexible Joint Robot Manipulator

Amjad J. Humaidi, Hussein M. Badr, and Ahmed R. Ajil

Abstract— **This work presents the design of active disturbance rejection control (ADRC) strategy to position control of a single-link flexible joint robot manipulator. Two schemes of ADRC are presented, Linear Active Disturbance Rejection Controller (LADRC) and Nonlinear Active Disturbance Rejection Controller (NADRC). A comparison study in terms of transient performances, robustness characteristics and disturbance rejection capabilities has been made based on LADRC and NADRC. The robustness of both controllers is evaluated by measuring the amount of deviation in system performance due to uncertainty in system parameters, One issue with NADRC and LADRC is they include various parameters and unless they are properly tuned, will have an adverse effect on the estimation process and in turn, on the system performance. The particle swarm technique (PSO) has been selected as an optimal tuner to improve the estimation process and thereby, to enhance the system performance.**

Keywords: ADRC, Flexible joint manipulator, PSO.

I. INTRODUCTION

In flexible joint robot manipulators, the elasticity of the transmission devices on the joints has been taken into account. Considering the effect of joint flexibility would develop a more exact model of industrial robot. However, a further complexity is added to the robot model, which raises a new control problem and therefore motivated the researchers in this relevant field further indulge.

In the past three decades many researchers have worked in the control of flexible joint robots. In [1], the sliding mode control strategy has been applied to a flexible joint manipulator. However, for feasible implementation of this control scheme, the control design requires the knowledge of uncertainty bounds and also the complete information of all system states. In [2], a dynamic feedback control design is developed for the trajectory tracking control problem of robotic manipulators with flexible joints. In this control design, the position measurements of the link and motor are needed, such that a reduced-order observer is used to estimate the required velocities for control. However, in this work, the establishment of system robustness requires certain conditions to be imposed on the uncertainties. In [3], the proposed control is based on a singular perturbation approach and the measurements of elastic force and position are prerequisites for the control design. This work suggested a nonlinear sliding state observer to estimate link velocities and elastic force time derivatives required for this control strategy. A control design based on the integral manifold formulation [4], adaptive control [5] and a back-stepping approach [6] are some other approaches reported in the literature. It has been seen that the majority of control designs in the literature require either information of complete states or at least the position state or some state on the motor side. Moreover, the guarantee of robustness may be highly dependent on the systems model and requires the knowledge of some characteristics of uncertainties.

Active Disturbance Rejection Controller (ADRC) was firstly proposed by J. Han with nonlinear gains. The control design of ADRC focused on nonlinear systems and considered both uncertain dynamics and disturbances. The essential idea of ADRC is firstly to combine both internal uncertain dynamics and external disturbances into a total uncertainty and to then estimate this combined uncertainty by an extended state observer (ESO) and thereafter to be cancelled out using state feedback structure. This renders ADRC applicable for many practical systems [7]. The Nonlinear ADRC (NADRC) has been parameterized and modified to linear ADRC (LADRC) with linearized gains by Z. Gao [8]. ADRC requires little information of the plant and is not completely dependent on the mathematical model of the system, which makes it very robust against system uncertainty [7].

Active Disturbance Rejection Control (ADRC) has recently attracted the interest of many researchers in robotics. A method using ADRC has been proposed for the control of a flexible joint robot in the control design, using cascade Nonlinear ADRC [9] and a feedback linearization (FL) based control law based upon ESO is presented in [10].

In the present work, two active disturbance rejection control schemes are presented, NADRC and LADRC, in order to control a single-link flexible joint robot manipulator; the work contribution can be highlighted by the following points:

- A performance comparison between linear and Nonlinear ADRC is made in terms of dynamic behavior and robustness capability.
- The suggested controls have to control the nonlinear system structure of the flexible joint manipulator without linearization.
- A second order ADRC has been used to control a fourth order system.
- The PSO technique is included to improve the closed-loop system performance.

A. J. Humaidi is with the Department of Control and Systems Engineering, University of Technology, Iraq, Baghdad (mobile: 964-790-1227676; e-mail: 601116@uotechnology.edu.iq).

H. M. Badr is with the Training and Energy Researches Office, Ministry of Electricity, Iraq, Baghdad (e-mail: cse.61104@uotechnology.edu.iq).

A. R. Ajil is with the Electrical Engineering Technical College, Middle Technical University, Baghdad, Iraq (e-mail: drahmed69@gmail.com).

II. JOINT FLEXIBILITY AND SYSTEM MODELING

Due to high complexity and nonlinearity of flexible joint manipulators, their modeling, simulation and real-time control is still a challenging and open problem. Their significant effect has attracted many academic and industrial researchers such that they dominated over link flexibility available nowadays. There are often seen in many applications where the harmonic gears drive industrial robotic manipulators [11].

The present work considers a single-link manipulator with a flexible joint operating in only vertical plane. The model of joint flexibility can be described by a torsional and linear spring as illustrated in Fig. 1. It is evident that the motor actuates the arm via a spring attached directly to the shaft of motor shaft [12].

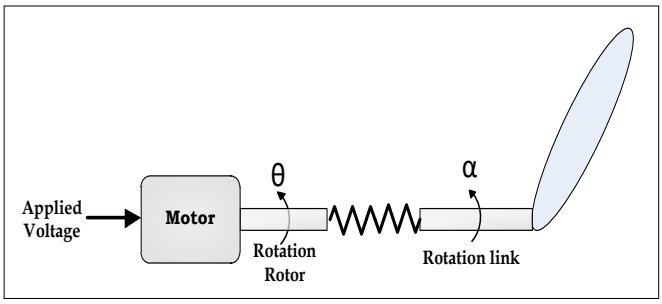

Fig.1 Flexible joint robot.

The development of mathematical model utilized the Lagrange method, which is basically based on conservation of energy and it can establish the model by calculating the difference between kinetic energy K and the potential energy P for all components of the flexible joint robot; i.e, [12]

$$L = K - P \tag{1}$$

Lagrange equations are configured as follows:

$$\frac{d}{dt}\frac{dL}{d\dot{\alpha}} - \frac{dL}{d\alpha} = 0 \tag{2}$$

$$\frac{d}{dt}\frac{dL}{d\dot{\theta}} - \frac{dL}{d\theta} = \tau \tag{3}$$

Based on Fig. 1, the following equations can be derived [12]:

$$J_\ell \ddot{\theta} + J_\ell \ddot{\alpha} + K_s \alpha - m\,g\,h\,\sin(\theta+\alpha) = 0 \tag{4}$$

$$(J_h + J_\ell)\ddot{\theta} + J_\ell \ddot{\alpha} - m\,g\,h\,\sin(\theta+\alpha) = \tau \tag{5}$$

Using Kirchhoff's Voltage Law (KVL) and neglecting the motor inductance, the electrical side of the system gives:

$$v = i\,R_m + K_m K_g\,\omega$$

$$i = (v/R_m) - (K_m K_g\ \omega/R_m) \tag{6}$$

Where ω is the angular velocity of the motor ($\dot{\theta} = \omega$), v is the applied input voltage, R_m is the armature resistance, K_m motor gain and K_g is the gear ratio. The current is related to developed torque τ by the following equation:

$$\tau = K_m K_g\, i \tag{7}$$

One can then deduce from Eq. (7) and (6) that:

$$\tau = \left(\frac{K_m K_g}{R_m}\right) v - \left(\frac{K_m^2 K_g^2}{R_m}\right)\omega \tag{8}$$

Substituting Eq. (4) into Eq. (5) yields

$$J_h \ddot{\theta} - K_s\,\alpha = \left(\frac{K_m K_g}{R_m}\right) v - \left(\frac{K_m^2 K_g^2}{R_m}\right)\omega \tag{9}$$

or,

$$\ddot{\theta} = \left(\frac{K_m K_g}{J_h R_m}\right) v - \left(\frac{K_m^2 K_g^2}{J_h R_m}\right)\dot{\theta} + \left(\frac{K_s}{J_h}\right)\alpha \tag{10}$$

From Eq. (9) and Eq. (4), one can get

$$\ddot{\alpha} = -\left(\frac{K_m K_g}{J_h R_m}\right) v + \left(\frac{K_m^2 K_g^2}{J_h R_m}\right)\dot{\theta} - \left(\frac{K_s}{J_h} + \frac{K_s}{J_\ell}\right)\alpha + \left(\frac{m\,g\,h}{J_\ell}\right) sin(\theta+\alpha)$$

The arm angle (tip angle) is composed of the sum α and θ. Letting $x_1 = \theta$, $x_2 = \alpha$, $x_3 = \dot{x}_1 = \dot{\theta}$, $x_4 = \dot{x}_2 = \dot{\alpha}$, then the system described by Eq. (9) and Eq. (10) can be written in state variable form [14]:

$$\dot{x}_1 = x_2$$

$$\dot{x}_2 = x_3$$

$$\dot{x}_3 = \left(\frac{K_m K_g}{J_h R_m}\right) v - \left(\frac{K_m^2 K_g^2}{J_h R_m}\right) x_3 + \left(\frac{K_s}{J_h}\right) x_2 \tag{11}$$

$$\dot{x}_4 = -\left(\frac{K_m K_g}{J_h R_m}\right) v + \left(\frac{K_m^2 K_g^2}{J_h R_m}\right) x_3 - \left(\frac{K_s}{J_h} + \frac{K_s}{J_\ell}\right) x_2 + \left(\frac{m\,g\,h}{J_\ell}\right)\sin(x_1 + x_2)$$

$$y = x_1 + x_2$$

III. ACTIVE DISTURBANCE REJECTION CONTROL

A. The structure of Nonlinear ADRC

In this structure, the Tracking Differentiator (TD) and the Nonlinear Extended State Observer (NESO) constitutes the main parts of nonlinear ADRC control. The tracking differentiator's function is to manage the transient process and in addition, if the input is corrupted by noise, then appropriate filters and a tracking differentiator are used to remove the noise effect. Fig.2 describes the basic elements of nonlinear ADRC.

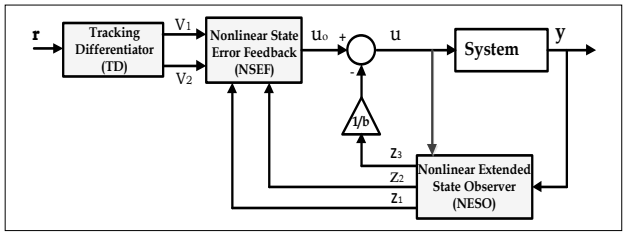

Fig. 2 A schematic representation of NADRC

The mathematical description of TD is generally given by [13]:

$$\dot{z}_1 = z_2$$

$$\dot{z}_2 = f_h$$

$$f_h = f_{han}(z_1 - v, z_2, r, h) \tag{12}$$

Where v is the input signal, r is called the speed factor, h is the filter factor and $f_{han}(x_1, x_2, r, h)$ is the integrated function of time optimum control, which is derived by:

$$f_{han} = \begin{cases} r.sign(a) & |y| > d \\ r\dfrac{a}{d} & |y| \le d \end{cases} \quad (13)$$

where,

$$a = \begin{cases} x_1 + \dfrac{(a_o - d)}{2} sign(y), & |y| > d_o \\ x_2 + \dfrac{y}{h}, & |y| \le d_o \end{cases} \quad (14)$$

$$d = r.h$$
$$d_o = h.d$$
$$y = x_1 + x_2.h$$
$$a_o = \sqrt{d^2 + 8.r.|y|}$$

For the position control of single-link flexible joint robot manipulator, the angle of flexible joint robot, z_1, track the angle of flexible joint robot, z_2, track the differential signal.

The other part of nonlinear ADRC is NESO, which was proposed by J. Han in 1995. It is characterized by an inherent robustness due to independency of a plant mathematical model. The model of NESO can be described by:

$$e = z_1 - y$$
$$\dot{z}_1 = z_2 - L_1.e$$
$$\dot{z}_2 = z_3 - L_2.fal(e, \alpha_1, \delta_1) + b.u \quad (15)$$
$$\dot{z}_3 = -L_3.fal(e, \alpha_2, \delta_2)$$

Where e is the error between actual and estimated output of system, L_1, L_2, L_3 represent the gains of observer, z_1, z_2 are the estimates of the states x_1 and x_2. The state variable z_3 is the estimate state of combined uncertain and nonlinearity disturbances (external and internal) of the system. The function $fal(e, \alpha, \delta)$ is a nonlinear function:

$$fal(e, \alpha, \delta) = \begin{cases} \dfrac{e}{\delta^{\alpha-1}}, & |e| \le \delta \\ |e|^{\alpha} sign(e), & |e| > \delta \end{cases}$$

where the δ is a small number parameter separating between linear and nonlinear regions. This number is nominally selected to be less than the maximum error. The parameter α describes the degree of nonlinearity in the nonlinear region of the fal-function and it is chosen to be in the range (0 and 1).

The Nonlinear State Error Feedback (NLSEF) is the other significant of NADRC structure. The mathematical form of NLSEF is described by:

$$e_1 = v_1 - z_1$$
$$e_2 = v_2 - z_2$$
$$u_o = k_p.fal(e_1, \alpha_1, \delta_1) + k_d.fal(e_2, \alpha_2, \delta_2) \quad (16)$$
$$u = u_o - \frac{z_3}{b}$$

Where e_1, e_2 represent the error between input signals and the estimate states of system, k_p, k_d are gains of NLSEF, $fal(e_1, \alpha_1, \delta_1)$, $fal(e_2, \alpha_2, \delta_2)$ are the nonlinear functions of NLSEF.

B. Structure of the Linear ADRC

The elements of LADRC structure consists mainly of Extended State Observer (ESO) and State Error Feedback (SEF). In this structure, the tracking differentiator has been excluded and, for the sake of simplicity in parameter tuning, NESO is replaced by Linear ESO (LESO), in which the *fal* function is linearly related to input error. The mathematical form of LESO can be written as;

$$e = y - z_1$$
$$\dot{z}_1 = z_2 + L_1.e$$
$$\dot{z}_2 = z_3 + L_2.e + b.u \quad (17)$$
$$\dot{z}_3 = L_3.e$$

where L_1, L_2 and L_3 are the observer gains and the variable z_3 stands for lumped disturbance and uncertainty, together with system nonlinearity. The other element of LARC scheme is LSEF, which can be described by the following set of equations:

$$e_1 = v_1 - z_1$$
$$e_2 = v_2 - z_2$$
$$u_o = k_p.e_1 + k_d.e_2 \quad (18)$$
$$u = u_o - z_3 / b$$

where e_1, e_2 represent the error between input signals and estimated states of system and k_p and k_d are the gains of linear state feedback (LSEF). Fig.4 shows the schematic diagram of Linear ADRC.

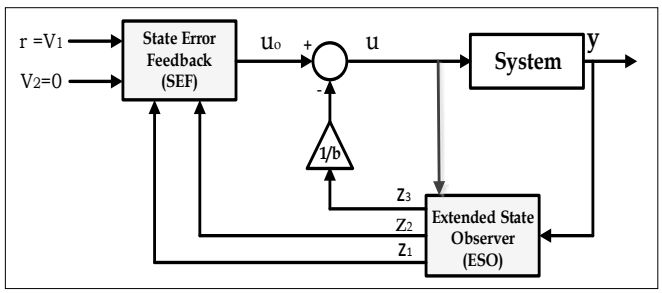

Fig. 3 A schematic representation of LADRC

C. ADRC-Based on PSO

The original ADRC system is characterized by having many design parameters. To improve the control capabilities, such parameters have to be tuned. Due to the complexity of ADRC scheme and tight coupling of parameters, the use of trial-and-error procedure is exhaustive and does not give global optimized solutions and hence a modern optimization algorithm is required. The present work suggested Particle

Swarm Optimization (PSO) technique for tuning the parameters of control strategy. The PSO algorithm is based on the behavior of swarm individuals. These individuals communicates information among themselves in such a manner which leads to increased efficiency of the group [14]. This optimization technique is not only a tuning tool for the parameters but also to search and find the best value of them. This can be achieved by evaluation and calculating the minimum error between desired and actual states.

Therefore, relying on PSO algorithm rather than trial-and-error procedure will better improve the process of state estimation and consequently the performance of closed-loop system dynamic is better enhanced due to improved estimates of observer. It is clear that LADRC has less number of parameters than that of NADRC. The numerical values presented in the above tables represent the optimal values of parameters, which are tuned based on estimation error minimization. The index of Root Mean Square Error (RMSE) has been suggested as a fitness function for evaluating the rapidity, stability and accuracy of the system.

$$J(RMSE)=\sqrt{\frac{\sum_{i=1}^{n} e^2}{n}}$$

A parameterization method proposed by Gao [8] is used to tune the parameters of LADRC. This parameterization method determines the gains value of both controller and observer, based on bandwidth of the observer ω_0 and control ω_c. This can be clarified using the relationship between controller gains and its bandwidth frequency ω_c :

$$\lambda(s)=s^2+k_d s+k_p=(s+\omega_c)^2$$

where, $k_d=2\omega_c$, $k_p=\omega_c^2$. Similarly, based on the following equation, which relates observer gains and its bandwidth, the observer gains can be obtained:

$$\lambda(s)=s^3+L_1 s^2+L_2 s+L_3=(s+\omega_0)^3$$

Where, $L_1=3\omega_0$, $L_2=3\omega_0^2$, $L_3=\omega_0^3$. Thus, this method could simplify the level of complexity to determine the optimal gain values of LESO and NESO, based on PSO. Table 1 lists the optimal parameters of NESO, NLSEF and TD, which have been tuned by the PSO algorithm. Alternately, Table I shows the optimal parameters of LESO and LSEF, resulting from the PSO optimizer.

TABLE I. Optimal parameters of NADRC

NESO. Param.	Value	NLSEF. Param.	Value	TD. Param.	Value
L_1	53.9	β_1	3.2324	h	0.000001
L_2	969.7	β_2	3.5958	r	8
L_3	5811.6	α_1	0.9		
b	46.3634	δ_1	0.00001		
α_1	1	α_2	1.25		
δ_1	0.1	δ_2	0.00001		
α_2	0.98				
δ_2	0.1				
α_3	0.78				
δ_3	0.1				

TABLE II. Optimal parameters of LADRC

LESO. Param.	Value	LSEF. Param.	Value
ω_o	17.979	ω_c	1.7979
L_1	53.9	β_1	3.2324
L_2	969.7	β_2	3.5958
L_3	5811.6		
b	46.3634		

IV. SIMULATED RESULTS

In this section, the dynamic behavior of a flexible-joint system, based on ADRC, is established using MATLAB/Simulink. The numeric values of system parameters are listed in Table III.

TABLE III. Numerical values of system parameters [12]

Parameter	Symbol	Value
Load Inertia	J_l	0.0059 [$kg.m^2$]
Inertia of hub	J_h	0.0021 [$kg.m^2$]
Link Mass	m	0.403 [kg]
Height of C.M.	h	0.06 [m]
Spring Stiffness	K_s	1.61 [N/m]
Motor Const.	K_m	0.00767
Gear Ratio	K_g	70
Motor Resist.	R_m	2.6 [Ω]
Gravity Const.	g	-9.81 [N/m]

The first comparison is made based on how well the transient characteristics could be given by such controllers. The controller reference input is assigned to be a step input of height 30^0 and the tip angle $\alpha+\theta$ is the output response, which have to be controlled. Fig. 4 shows the dynamic behaviors of a flexible-joint system resulting from both controllers. The figure shows that NADRC offer better transient characteristics than LADRC. Table (4) makes a quantitative comparison based on simulation, which confirms that the response due to NLADRC outperforms the response resulting from LADRC. The key index of comparison is measured by root means square error (RMSE), which calculate the root mean square of error over the entire response. The response with less RMSE will address the best controller.

TABLE IV. Dynamic performance report of controllers

Controller	RMSE	Maximum overshoot %	Settling Time (sec.)
LADRC	9.7576	3.8	7.133
NADRC	2.9558	2.93	1.54

Another comparison is made to assess the robustness capabilities of the suggested controllers due to changes of system parameters. Two uncertainties are permitted to appear in the present work; internal uncertainty, represented by changing link mass and center of mass and external uncertainty given by disturbance exertion. Fig. 5 and Fig. 6 show the dynamic responses of tip angle and control signals resulting from LADRC and NLADRC, respectively. The responses indicated in the figures correspond to three values of masses (nominal value of mass, two times nominal value of mass, three times nominal value of mass). On the other hand, Fig.7

and Fig. 8 show the transient responses of tip angle and control signals due to LADRC and NLADRC, respectively, and under a change of mass center (h). In this scenario, two cases of mass centers have been addressed; the nominal value and 10% deviated value (from the nominal).

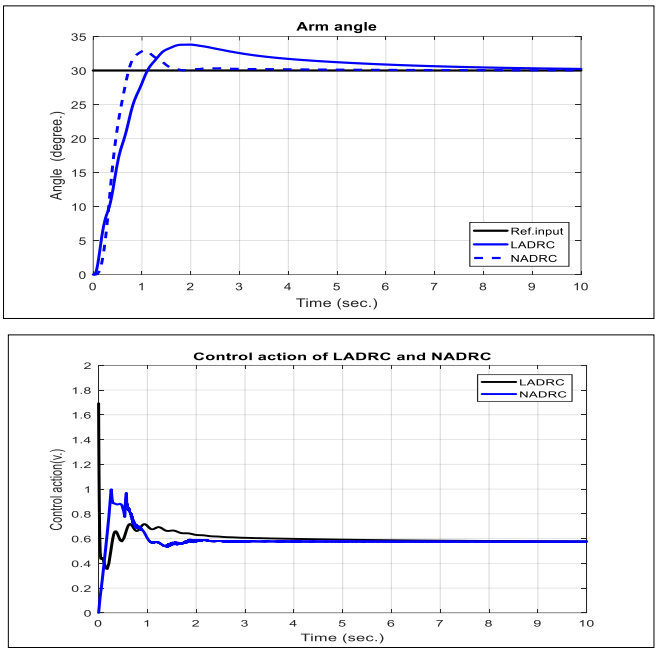

Fig. 4 Performance of NADRC and LADRC with nominal case

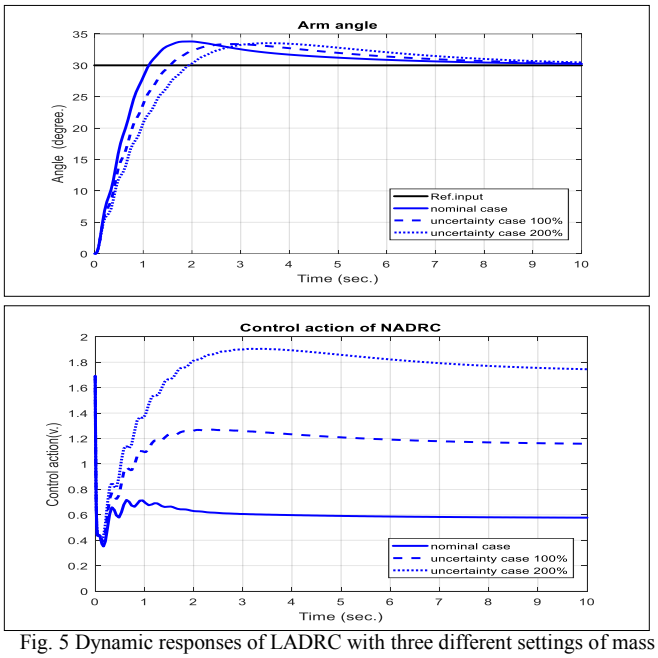

Fig. 5 Dynamic responses of LADRC with three different settings of mass

The next simulations are dedicated for evaluation of disturbance rejection capability of both controllers. The disturbance is injected as angle perturbation between time 7-7.2 seconds with height of 20^0.

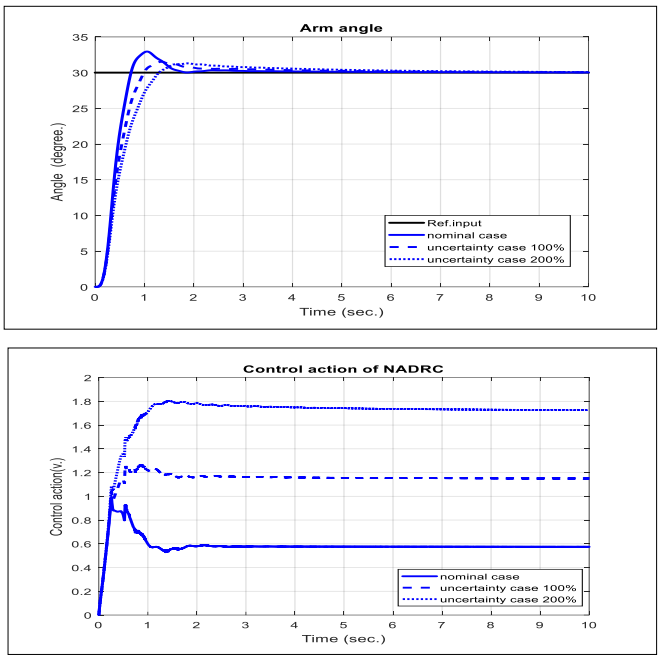

Fig. 6 Dynamic responses of NADRC with three different setting of mass

Table (5) gives a summary of robustness characteristics for both controllers. The table reports the deviation in transient response from the nominal case, measured in RMSE, when the system is subjected to parameter variations (change in mass, change in the length of C.M). It is evident from the table that the minimum deviation from the nominal occurs with LADRC and this indicates that this controller have better robustness characteristics than NLADRC. In Table (5), the disturbance rejection capability of both controllers are evaluated in terms of how the response has been deviated upon abrupt disturbance change. RMSE measure is also used here to quantify the deviation. It is clear from the table that LADRC has better disturbance rejection capability than its opponent.

TABLE V. Robustness evaluation of controllers

Percentage change of system parameters	Percentage Change from nominal	
	LADRC	NADRC
+100% of nominal mass	2.9444 %	10.9683 %
+200% of nominal mass	6.6348 %	32.9454 %
+10% of nominal C.M	0.3105 %	2.5746 %

V. Conclusion

This paper presents a comparison study between two active rejection disturbance controllers in terms of transient characteristics and robustness. Based on simulated results, one can conclude that NLADRC offer better dynamic behavior than LADRC under nominal condition. However, LADRC possesses better robustness characteristics than NLADRC when the system is subjected to a variation of parameters and sudden change in disturbance. PSO has played a vital role in optimization and performance enhancement of an overall active rejection disturbance controlled system.

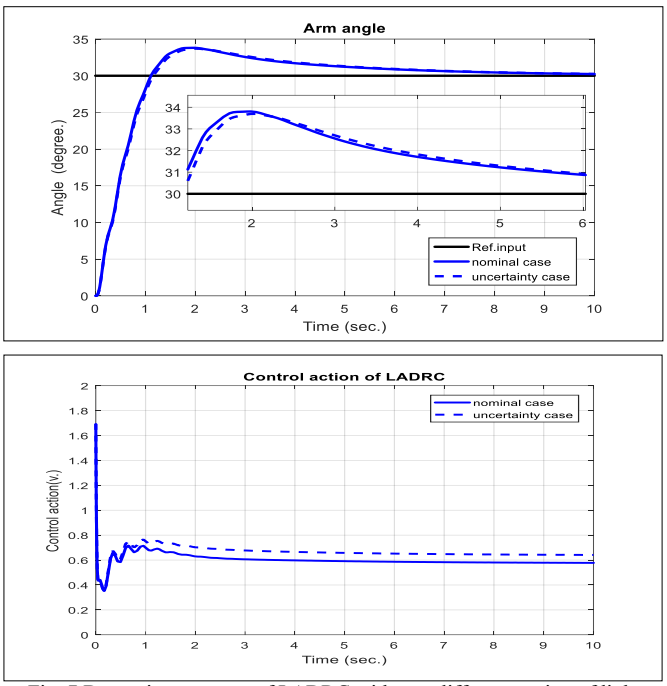

Fig. 7 Dynamic responses of LADRC with two different setting of link Length

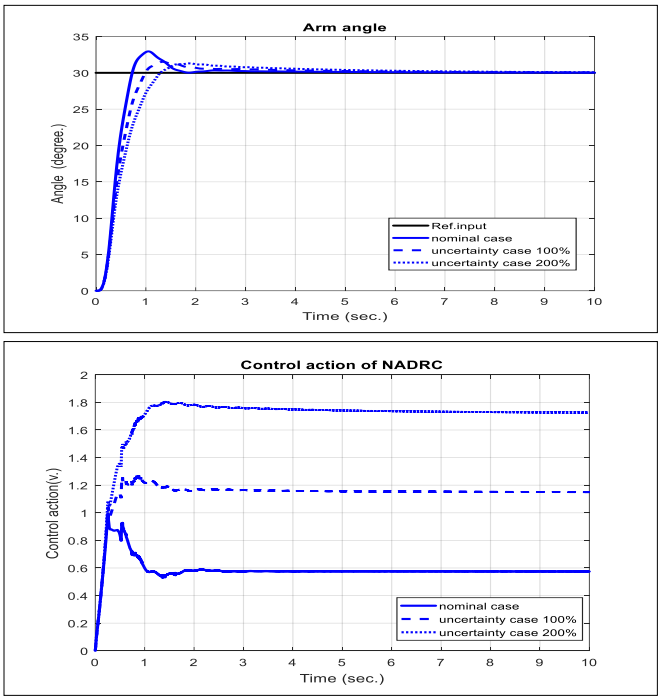

Fig. 8 Dynamic responses of LADRC with two different setting of link length

REFERENCE

[1] S. K. Spurgeon, L. Yao, and X. Y. Lu, “Robust tracking via sliding mode control for elastic joint manipulators,” Proc. Inst. Mech. Eng. I, vol. 215, no. 4, pp. 405–417, 2001.

[2] Y. C. Chang, B. S. Chen, and T. C. Lee, “Tracking control of flexible joint manipulators using only position measurements,” Int. J. Control, vol. 64, no. 4, pp. 567–593, 1996.

[3] J. Hernandez and J.-P. Barbot, “Sliding observer-based feedback control for flexible joints manipulator,” Automatica, vol. 32, no. 9, pp. 1243–1254, Sep. 1996.

[4] M. W. Spong, “Modeling and control of elastic joint robots,” Trans. ASME, J. Dyn. Syst., Meas., Control, vol. 109, no. 4, pp. 310–319, Dec. 1987.

[5] F. Ghorbel, J. Y. Hung, and M. W. Spong, “Adaptive control of flexible joint manipulators,” IEEE Control Syst. Mag., vol. 9, no. 7, pp. 9–13, Dec. 1989.

[6] J. Oh and J. Lee, "Control of Flexible Joint Robot System by Backstepping Design Approach," Intelligent Automation & Soft Computing, vol. 5, no. 4, pp. 267-278, 1999.

[7] J. Han, "From PID to Active Disturbance Rejection Control", IEEE Transactions on Industrial Electronics, vol. 56, no. 3, pp. 900-906, 2009.

[8] Z. Gao, "Scaling and bandwidth-parameterization based controller tuning", Proceedings of the 2003 American Control Conference, 2003., vol. 6, no. 7, pp. 4989 - 4996, 2003.

[9] Amjad J. Humaidi, Hussain M. Bad, Akram H. Hameed "PSO-Based Active Disturbance Rejection Control for Postion Control of Magnetic Levitation System," 5th international conference on Control, Decision and Information Technologies (CoDIT'18), Thessaloniki, Greece, April 10-13, 2018.

[10] S. Talole, J. Kolhe and S. Phadke, "Extended-State-Observer-Based Control of Flexible-Joint System with Experimental Validation", IEEE Transactions on Industrial Electronics, vol. 57, no. 4, pp. 1411-1419, 2010.

[11] B. Siciliano and O. Khatib, Springer handbook of robotics. Berlin: Springer, pp. 287-295, 2008.

[12] A. Dehghani and H. Khodadadi, "Self-Tuning PID Controller Design Using Fuzzy Logic for Single-Link Flexible Joint Robot Manipulator", Jurnal Teknologi, vol. 78, no. 6-13, 2016.

[13] F. Meng, J. Yang, P. Yang and B. Sun, "The Research of Frequency Characteristics of Tracking Differentiator", Applied Mechanics and Materials, vol. 182-183, pp. 1474-1478, 2012.

[14] Z. Gaing, "A Particle Swarm Optimization Approach for Optimum Design of PID Controller in AVR System", IEEE Transactions on Energy Conversion, vol. 19, No. 2, pp. 384-391, 2004.